Notes on x-ray wave-field forward model

Scott Trinkle

Last edited: March 18, 2019

Introduction

In these notes, I follow the various derivations in Paganin [1] chapters 1 and 2, tracing the propagation of a coherent x-ray wavefield through a scattering object and to a detector. The goal is to write down a physical imaging forward model that is as rigorous as possible, in order to simulate and/or predict the phase effects we have observed in our high-absorbing samples.

This problem will be addressed in two stages:

1. Propagation of an incoming synchrotron x-ray wave-field $\Psi(x, y, z, t)$ through a scattering object with frequency-dependent, complex index of refraction $n_\omega(x, y, z)$ that exists between planes $z = 0$ and $z = z_0$ along the optical axis, z.

2. Propagation of the scattered wave-field from the exit-plane $z = z_0$ to the detector plane $z = z_0 + \Delta$, and calculation of the detected intensity: $I(x, y, z_0 + \Delta) = |\Psi(x, y, z = z_0 + \Delta)|^2$

In these notes, I am restricting myself to modeling a single 2D projection of the object, which I leave in terms of the complex, 3D index of refraction: $n_\omega(x, y, z)$ for now.[1] The extension to 3D tomographic imaging will be explored later (I expect that existing tomographic techniques will generally be appropriate once we understand the 2D phase effect). Note that these notes will also neglect the effects of incoherent scattering.

I will document all simplifying approximations and assumptions made in the various derivations presented in these notes. The results will be used to construct a computational framework that can simulate imaging of realistic digital phantoms in various imaging geometries. These studies can be used to understand the validity of different assumptions for our imaging task, which will be useful as we go on to look at appropriate ways of linearizing and inverting our model.

1 Propagation through matter

In this section, we consider the propagation of an incoming, complex monochromatic wave-field $\psi_\omega(x, y, z)$ from left to right through an object parameterized by the frequency-dependent complex index of refraction $n_\omega(x, y, z)$ (the extension to polychromatic wave-fields is discussed in section 1.1 below). Figure 1 illustrates the scattering geometry to be used throughout these notes.

1.1 Inhomogeneous Helmholtz equation

In section 2.1, Paganin starts with Maxwell's equations and develops the relevant scalar wave equation in the presence of scatterers. A number of typical assumptions are made; I am listing them here, indexed by the relevant equation number:

- (2.5–2.8) The scattering material is linear and isotropic. That is: $\boldsymbol{D} = \epsilon \boldsymbol{E}$ and $\boldsymbol{B} = \mu \boldsymbol{H}$ where $\boldsymbol{D}$ is the electric displacement, $\boldsymbol{B}$ is the magnetic induction, $\boldsymbol{E}$ is the electric field, $\boldsymbol{H}$ is the magnetic field, ϵ is the electric permittivity

[1] See Appendix A for a discussion of the relationship between $n_\omega(x, y, z)$ and additional physical parameters

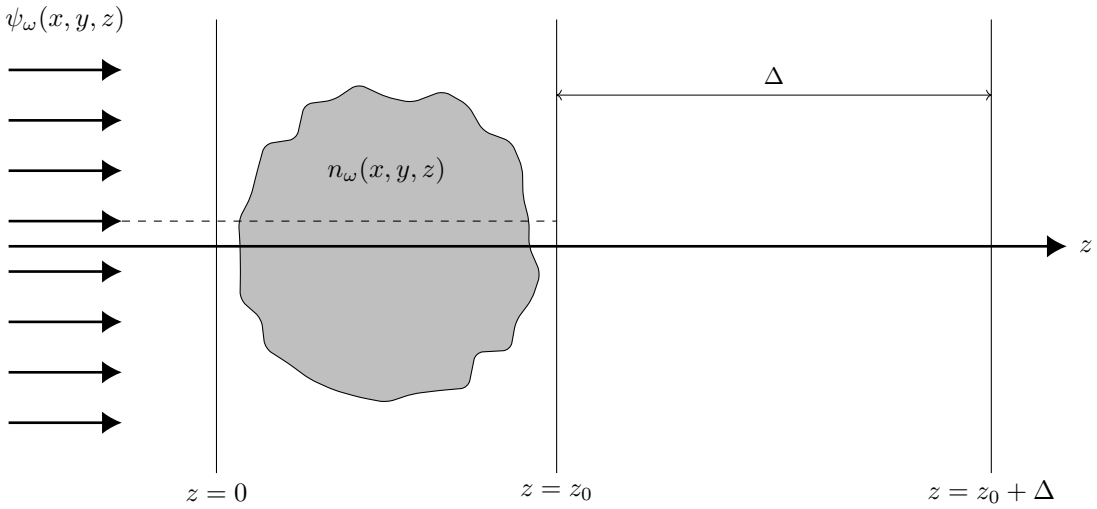

Figure 1: A z-directed monochromatic plane wave ψ_ω is indicated by the arrows at the left of the diagram. All scatterers lie between $z = 0$ and $z = z_0$.

and μ is the magnetic permeability. This assumptions thus excludes ferroelectric and ferromagnetic materials, for example.

- (2.13) The material is static, so both μ and ϵ are both independent of time.
- (2.18–2.19) The material is non-magnetic, that is: $\mu(x, y, z) = \mu_0$, where μ_0 is the permeability of free space. In other words, we assume our metal stains have very low magnetic susceptibility. I am assuming this is a fair, typical assumption for most x-ray imaging tasks — a cursory Wikipedia search puts the susceptibility of osmium at $11{\times}10^{-6}$ cm^{-3}/mol, which seems relatively low compared to other listed metals (aluminum is at $1.7{\times}10^{-5}$ cm^{-3}/mol, for instance).
- (2.18–2.19) There are no charge or current densities: $\rho(x, y, z, t) = 0$ and $\boldsymbol{J}(x, y, z, t) = \mathbf{0}$.
- (2.20–2.21) Scatterers are "sufficiently slowly varying" over length scales comparable to the wavelength of the x-ray radiation. At 20 keV, our wavelength is around 6×10^{-11} m — it is fair to assume our samples are slowly varying over this length scale.

Under these assumptions, a complex scalar, electromagnetic wave $\Psi(x, y, z, t)$ can be represented as a Fourier integral over non-negative angular frequencies ω:

$$\Psi(x, y, z, t) = \frac{1}{\sqrt{2\pi}} \int_0^\infty \psi_\omega(x, y, z) \, \exp(-i\omega t) \, \mathrm{d}\omega, \tag{1}$$

whose spatial monochromatic components $\psi_\omega(x, y, z)$ obey the "inhomogeneous" Helmholtz equation:

$$\left[\nabla^2 + k^2 n_\omega^2(x, y, z)\right] \psi_\omega(x, y, z) = 0, \tag{2}$$

where k is the wavenumber $(2\pi/\lambda)$ and $n_\omega(x, y, z)$ is the complex, frequency-dependent refractive index of the scatterer, given by:

$$n_\omega(x, y, z) = c\sqrt{\epsilon_\omega(x, y, z)\mu_0} = \sqrt{\frac{\epsilon_\omega(x, y, z)}{\epsilon_0}}. \tag{3}$$

It is appropriate, then, to develop solutions to equation 2 for each monochromatic component ψ_ω, then use equation 1

to construct the full wave-field. This will be the strategy throughout these notes. The remainder of this section will detail a number of methods for solving this equation under different approximations.

1.2 Projection approximation

In section 2.2, Paganin reviews the projection approximation. With reference to Figure 1, we use a cartesian coordinate frame and consider a monochromatic plane wave $\psi_\omega(x, y, z)$ propagating from left to right along the optical axis z. The object exists within the space $0 < z < z_0$, with all other space being vacuum. In a ray optics framework, the projection approximation assumes that "the scatterers are sufficiently weak so as to negligibly perturb the ray paths which would have existed in the volume occupied by the scatterer had the scatterer been absent." Effectively, the phase and amplitude of the disturbance at the surface $z = z_0$ can be expressed in terms of the phase and amplitude shifts accumulated along a given ray path connecting the entrance and exit surfaces, with the ray paths being the same as if the scattering object was absent (one such path is illustrated by the dotted line through the object in Figure 1).

We begin by modeling the wave as the product of an unscattered plane wave $\exp(ikz)$ with an envelope $\tilde{\psi}_\omega(x, y, z)$:

$$\psi_\omega(x, y, z) = \tilde{\psi}_\omega(x, y, z) \exp(ikz), \tag{4}$$

noting that $|\tilde{\psi}_\omega(x, y, z)|^2 = |\psi_\omega(x, y, z)|^2$. Equation 2 can then be expanded in terms of the envelope $\tilde{\psi}_\omega$:

$$\left\{ 2ik\frac{\partial}{\partial z} + \nabla_\perp^2 + \frac{\partial^2}{\partial z^2} + k^2 \left[n_\omega^2(x, y, z) - 1 \right] \right\} \tilde{\psi}_\omega(x, y, z) = 0, \tag{5}$$

where

$$\nabla_\perp^2 \equiv \frac{\partial^2}{\partial x^2} + \frac{\partial^2}{\partial y^2} \tag{6}$$

The development of the projection approximation then rests on the following assumptions:

- We can neglect the $\partial^2/\partial z^2$ term in equation 5. This amounts to the paraxial approximation, which I believe is fair for our synchrotron beam.
- We can also neglect the $\nabla_\perp^2$ term, as this is the only term that couples neighboring ray trajectories. Paganin does not go into any more detail on the conditions under which this is valid, besides that we are assuming "the scattering is sufficiently weak."

From here, we can solve equation 5 and write the wave-field at the exit surface $z = z_0$ in terms of that at the entrance surface $z = 0$:

$$\tilde{\psi}_\omega(x, y, z_0) \approx \exp\left\{ \frac{k}{2i} \int_0^{z_0} \left[1 - n_\omega^2(x, y, z) \right] \mathrm{d}z \right\} \tilde{\psi}_\omega(x, y, z = 0). \tag{7}$$

Define the complex, 2D projection of $1 - n_\omega^2$ as:

$$A_\omega(x, y) \equiv \int_0^{z_0} \left[1 - n_\omega^2(x, y, z) \right] \mathrm{d}z. \tag{8}$$

Then the full expression for the wave-field at the exit surface can be written, with reference to equation 4:

$$\psi_\omega(x, y, z_0) \approx \exp\left\{ \frac{-ik}{2} A_\omega(x, y) \right\} \tilde{\psi}_\omega(x, y, z = 0) \exp\left(ikz_0 \right). \tag{9}$$

Note, see Appendix A for discussion on a physical density-based parameterization of the object under the projection approximation.

1.3 The first Born approximation

In section 2.3–2.4, Paganin develops an integral-equation formulation of the differential inhomogeneous Helmholtz equation (equation 2) in terms of the outgoing Green function:

$$\psi_\omega(\boldsymbol{r}) = \psi^0_\omega(\boldsymbol{r}) - \frac{k^2}{4\pi}\iiint G_\omega(\boldsymbol{r}-\boldsymbol{r}')\left[1-n^2_\omega(\boldsymbol{r}')\right]\psi_\omega(\boldsymbol{r}')d\boldsymbol{r}', \tag{10}$$

where

$$\begin{aligned}\boldsymbol{r} &\equiv (x,y,z)\\ \boldsymbol{r}' &\equiv (x',y',z')\\ \psi^0_\omega(\boldsymbol{r}) &\equiv \text{ unscattered wave}\\ G_\omega(\boldsymbol{r}) &\equiv \frac{\exp(ik|\boldsymbol{r}|)}{|\boldsymbol{r}|}\end{aligned}$$

In section 2.5, Paganin then introduces the first Born approximation, in which you assume that the x-ray disturbance is "only slightly different from the disturbance that would have existed at each point $\boldsymbol{r}'$ in the volume in the absence of the scatterer." Effectively, this amounts to replacing $\psi_\omega(\boldsymbol{r}')$ with $\psi^0_\omega(\boldsymbol{r}')$ in the integral in the right side of equation 10:

$$\psi_\omega(\boldsymbol{r}) \approx \psi^0_\omega(\boldsymbol{r}) - \frac{k^2}{4\pi}\iiint G_\omega(\boldsymbol{r}-\boldsymbol{r}')\left[1-n^2_\omega(\boldsymbol{r}')\right]\psi^0_\omega(\boldsymbol{r}')d\boldsymbol{r}'. \tag{11}$$

This transforms equation 10 from an integral equation to an approximate integral expression for the total wave-field. This corresponds to a single-scattering approximation, in which each point in the scatterer emanates spherical waves with strength proportional to the wave incident at each point. The scatterer is assumed to be weak enough that the incident field is equal to the unscattered field.

In section 2.5.2, Paganin uses a Fourier integral representation of the Green function in order to develop a specific formulation of equation 11, calculating the wave-field at any $z > z_0$ for an incoming monochromatic plane wave: $\exp(i\boldsymbol{k}_0\cdot\boldsymbol{r})$, incident upon a slab of scatterers defined within $0 < z < z_0$:

$$\psi_\omega(\boldsymbol{r}) \approx \exp(i\boldsymbol{k}_0\cdot\boldsymbol{r}) - \frac{ik^2}{8\pi^2}\iint \mathrm{d}k_x\mathrm{d}k_y \frac{\exp\left[i\left(k_x x + k_y y + z\sqrt{k^2-k_x^2-k_y^2}\right)\right]\Gamma(\boldsymbol{k}_0,k_x,k_y)}{\sqrt{k^2-k_x^2-k_y^2}}, \quad z > z_0. \tag{12}$$

$$\Gamma(\boldsymbol{k}_0,k_x,k_y) \equiv \iiint \mathrm{d}\boldsymbol{r}'\left[1-n^2_\omega(\boldsymbol{r}')\right]\exp(i\boldsymbol{k}_0\cdot\boldsymbol{r}')\exp\left[-i\left(k_x x' + k_y y' + z'\sqrt{k^2-k_x^2-k_y^2}\right)\right] \tag{13}$$

1.3.1 Comment on implementation

Here, I extend the formulation of the first Born approximation in equations 12–13 to a form that can be written more compactly and implemented relatively simply. In our case, the incoming plane wave is aligned with the optical axis z, so we know that $\boldsymbol{k}_0 = (0,0,k)$ and $\boldsymbol{k}_0\cdot\boldsymbol{r} = kz$. First, for notational convenience, we define:

$$\zeta \equiv \sqrt{k^2-k_x^2-k_y^2}. \tag{14}$$

Since we know that $\left[1-n^2_\omega(\boldsymbol{r}')\right] = 0$ outside the scatterer, the integral in equation 13 is only nonzero for $0 < z < z_0$. We can thus write it as:

$$\Gamma(k_x,k_y) \equiv \iint \mathrm{d}x'\mathrm{d}y'\,\exp\left[-i\left(k_x x' + k_y y'\right)\right]\int_0^{z_0}\mathrm{d}z'\,\left[1-n^2_\omega(x',y',z')\right]\exp\left[iz'(k-\zeta)\right]. \tag{15}$$

This expression appears similar to a 2D Fourier transform of the z-projection of $\left[1-n^2_\omega(x',y',z')\right]$ with respect to x' and y'.

Note, however, that the $\exp\left[iz'(k-\zeta)\right]$ term in the z-projection couples the two conjugate variable pairs (x', y') and (k_x, k_y), so this is *not* a Fourier transform, strictly speaking. For compactness, we represent the action of equation 15 with the operator $\mathcal{A}_k$, where

$$\mathcal{A}_k n_\omega(x,y,z) \equiv \Gamma(k_x,k_y) = \iint \mathrm{d}x\mathrm{d}y \, \exp\left[-i\left(k_x x + k_y y\right)\right] \int_0^{z_0} \mathrm{d}z \, \left[1 - n_\omega^2(x,y,z)\right] \exp\left[iz(k-\zeta)\right]. \tag{16}$$

Now we note that the integral in equation 12 can be seen as the inverse Fourier transform of $\Gamma(k_x, k_y)$ after multiplication with a filtering factor $\exp\left[iz\zeta\right]/\zeta$ (the Fourier transform conventions used in these notes are given in Appendix B). The whole expression for the wave-field at some plane $z > z_0$ can thus be written compactly as

$$\psi_\omega(x,y,z) \approx \exp(ikz) - \frac{ik^2}{4\pi}\mathcal{F}^{-1}\left[\frac{\exp\left(iz\zeta\right)}{\zeta}\right]\mathcal{A}_k n_\omega(x,y,z), \quad z > z_0, \tag{17}$$

where cascaded operators act from right to left. This can be used to solve for the wave-field at both the exit plane $z = z_0$ and the detector plane $z = z_0 + \Delta$.

1.4 Born series

In section 2.6, Paganin extends the first Born approximation to a series of higher order Born approximations. First, we can write the distribution of refractive index in the scatterer as

$$\nu_\omega(\boldsymbol{r}) \equiv \frac{k^2}{4\pi}\left[n_\omega^2(\boldsymbol{r}) - 1\right], \tag{18}$$

and define the "Green operator" $\mathcal{G}_\omega$, such that:

$$\mathcal{G}_\omega f(\boldsymbol{r}) \equiv \iiint G_\omega(\boldsymbol{r} - \boldsymbol{r}') f(\boldsymbol{r}') \mathrm{d}\boldsymbol{r}', \tag{19}$$

for some function $f(\boldsymbol{r})$.

The first Born approximation can then be written:

$$\psi_\omega^{(1)}(\boldsymbol{r}) \approx \left[1 + \mathcal{G}_\omega \nu_\omega(\boldsymbol{r})\right] \psi_\omega^0(\boldsymbol{r}). \tag{20}$$

In this way, a "Born series" can be generated by iteratively using lower order Born estimates on the right side of equation 20:

$$\psi_\omega^{(m)}(\boldsymbol{r}) = \left\{1 + \mathcal{G}_\omega \nu_\omega(\boldsymbol{r}) + \left[\mathcal{G}_\omega \nu_\omega(\boldsymbol{r})\right]^2 + ... + \left[\mathcal{G}_\omega \nu_\omega(\boldsymbol{r})\right]^m\right\} \psi_\omega^0(\boldsymbol{r}). \tag{21}$$

1.5 Multislice approximation

In section 2.7, Paganin discusses the multislice approximation, which amounts to considering the effects of free-space propagation together with the projection approximation. In calculating the evolution of the wavefield from planes $z = z_1$ to $z = z_1 + \delta z$ in the scatterer, where $0 < z_1 < z_1 + \delta z < z_0$, we can use equation 7 to write:

$$\psi_\omega(x,y,z = z_1 + \delta z) \approx \mathcal{D}_{\delta z}\left(\exp\left\{\frac{k}{2i}\int_{z_1}^{z_1+\delta z}\left[1 - n_\omega^2(x,y,z)\right]\mathrm{d}z\right\}\psi_\omega(x,y,z = z_1)\right), \tag{22}$$

where $\mathcal{D}_{\delta z}$ is the free-space propagator, to be defined in section 2.1. By recursively applying the above equation from one plane to another in the scattering volume, one will arrive at the wave-field at the exit surface. In practice, the slice thickness δz is reduced until further reduction causes no appreciable change in the exit wave-field.

2 Propagation to detector

Having propagated the wave-field through the scattering object, we now turn our attention to the propagation of the exit wave-field through free space from plane $z = z_0$ to $z = z_0 + \Delta$.

In section 1.2, Paganin traces the development from Maxwell's equations to the Helmholtz equation for free space:

$$(\nabla^2 + k^2)\psi_\omega(x, y, z) = 0. \tag{23}$$

This development required no additional assumptions. The rest of this section will detail various ways of solving this equation.

2.1 Free space propagator

Paganin section 1.3 details the development of a free-space propagator using an angular spectrum formalism. Assuming all wave components are "forward-propagating" in vacuum, given the value of a wave-field at plane $z = z_0$, we can calculate the diffracted wave-field at plane $z = z_0 + \Delta$ with

$$\psi_\omega(x, y, z = z_0 + \Delta) = \mathcal{D}_\Delta \psi_\omega(x, y, z = z_0), \quad \Delta \geq 0 \tag{24}$$

where

$$\mathcal{D}_\Delta = \mathcal{F}^{-1} \exp\left[i\Delta\sqrt{k^2 - k_x^2 - k_y^2}\right]\mathcal{F}. \tag{25}$$

Again, $\mathcal{F}$ denotes a 2D Fourier transform, and cascaded operators act from right to left. This forms an exact solution to equation 23.

2.2 Fresnel diffraction

In section 1.4, Paganin develops the "Fresnel propagator" as a limiting approximation of the exact, free-space propagator given in equation 25. In the case that the wave-field is paraxial — that is, when all non-negligible plane-wave components of the field make a small angle with respect to a given optical axis — both $|k_x|$ and $|k_y|$ will both be much less than k_z. In this case, we can make the binomial approximation:

$$\sqrt{k^2 - k_x^2 - k_y^2} \approx k - \frac{k_x^2 + k_y^2}{2k}, \tag{26}$$

and write the diffraction operator as:

$$\mathcal{D}_\Delta \approx \exp(ik\Delta)\,\mathcal{F}^{-1} \exp\left[\frac{-i\Delta\left(k_x^2 + k_y^2\right)}{2k}\right]\mathcal{F}. \tag{27}$$

As in equation 24, the value of a wave-field at the plane $z = z_0 + \Delta$ can thus be written by applying this operator to the wave-field at plane $z = z_0$. Fresnel diffraction can also be written in terms of a convolution with the following kernel:

$$P(x, y, \Delta) = -\frac{ik\,\exp(ik\Delta)}{2\pi\Delta} \exp\left[\frac{ik(x^2 + y^2)}{2\Delta}\right]. \tag{28}$$

2.2.1 Sufficiency of Fresnel approximation

Paganin makes the following note about a sufficiency condition for making the Fresnel approximation:

> "As a sufficient condition for this to be so, we may demand that $k_x^2 + k_y^2 \ll k^2$, for the largest value of $k_x^2 + k_y^2$ for which $\mathcal{F}\psi_\omega(x, y, z = 0)$ is non-negligible in modulus. Denote this maximum value of $k_x^2 + k_y^2$ by $k_{max}^2 \equiv (2\pi/a)^2$,

where a represents the smallest non-negligible length scale present in the unpropagated disturbance...one arrives at the condition $a \gg \lambda$...[this] amounts to the statement that the smallest characteristic length scale, over which the unpropagated disturbance varies appreciably, is much larger in size than the wavelength of the radiation."

Again, our radiation has a wavelength on the order of 10^{-11} m — we do not expect our wave-fields to show appreciable variation on this length scale.

2.2.2 Comment on Fresnel number and "near" vs "far" field

A number of phase retrieval schemes make assumptions on the imaging geometry using the terms "near", "intermediate", or "far" fields. This can be related to the concept of the Fresnel number, N_F, defined as:

$$N_F = \frac{h^2}{\lambda \Delta}, \tag{29}$$

where h is the object feature size, Δ is the propagation distance, and λ is the wavelength. The terms "near", "intermediate" and "far" indicate $N_F \gg 1$, $N_F \sim 1$, and $N_F \ll 1$, respectively.

As motivation for this distinction, Paganin develops an expression for Fraunhofer diffraction in section 1.5. Consider the following integral expression for Fresnel diffraction:[2]

$$\psi_\omega(x, y, z = \Delta) = -\frac{ik \exp(ik\Delta)}{2\pi\Delta} \exp\left[\frac{ik}{2\Delta}\left(x^2 + y^2\right)\right] \iint \psi_\omega(x', y', z = 0) \exp\left[\frac{ik}{2\Delta}\left(x'^2 + y'^2\right)\right] \exp\left[\frac{-ik}{\Delta}\left(xx' + yy'\right)\right] \mathrm{d}x' \mathrm{d}y'. \tag{30}$$

If the propagation distance Δ is sufficiently large that the Fresnel number is less than unity: $N_F \ll 1$, then the first exponent in the integrand can be ignored:

$$\exp\left[\frac{ik}{2\Delta}\left(x'^2 + y'^2\right)\right] \approx 1, \tag{31}$$

and we have an expression for far-field, or "Fraunhofer" diffraction:

$$\psi_\omega(x, y, z = \Delta) = -\frac{ik \exp(ik\Delta)}{2\pi\Delta} \exp\left[\frac{ik}{2\Delta}\left(x^2 + y^2\right)\right] \iint \psi_\omega(x', y', z = 0) \exp\left[\frac{-ik}{\Delta}\left(xx' + yy'\right)\right] \mathrm{d}x' \mathrm{d}y'. \tag{32}$$

Note that the h^2 term in equation 29 is being represented by the $(x'^2 + y'^2)$ term in the integral. Accordingly, this term is related to the maximum beam width or imaging field of view — there will be some (x', y') for which $\psi_\omega(x', y', z = 0)$ is negligible and the integral is zero. The beam width at the synchrotron is on the order of $h \approx 1.5$ mm. We also know that $\lambda \approx 6 \times 10^{-11}$ m. Figure 2 shows the resulting Fresnel number as a function of Δ: We see that with these values, $N_F \gg 1$ for reasonable propagation distances, indicating that we are safe to assume we are in the "near" field regime.

3 Conclusion

We are now ready to write down a full forward-model for our imaging system using (admittedly loose) operator notation:

$$I_\omega(x, y, z = z_0 + \Delta) = \left| \mathcal{D}_\Delta^{(\mathrm{fs})} \mathcal{D}_{z_0}^{(\mathrm{sc})} n_\omega(x, y, z) \right|^2. \tag{33}$$

Here, $n_\omega(x, y, z)$ is the 3D, complex, frequency-dependent index of refraction of a scattering object defined between the planes $z = 0$ and $z = z_0$. $\mathcal{D}_{z_0}^{(\mathrm{sc})}$ is a diffraction operator that propagates an incoming monochromatic wave-field $\psi_\omega(x, y, z = 0)$ through the scattering object to the plane $z = z_0$. This could take the form of a number of approximations

[2] Note that this expression is propagating a wave-field a distance Δ through free space from the plane $z = 0$, rather than from $z = z_0$ as I have been using in these notes.

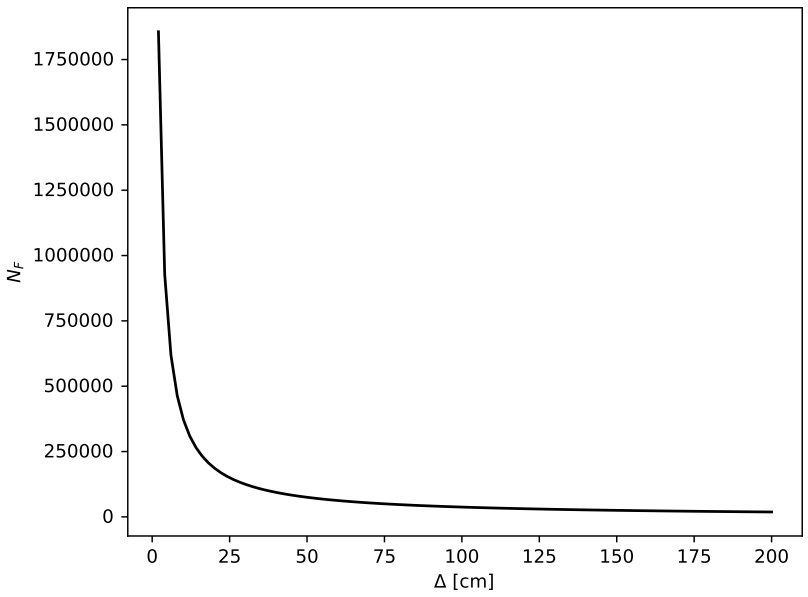

Figure 2: Fresnel number as a function of propagation distance.

discussed in these notes: namely equations 9 (projection), 17 (first Born), 21 (Born series), or 22 (multislice). $\mathcal{D}_{\Delta}^{(\mathrm{fs})}$ is an additional diffraction operator that propagates the scattered wave-field a distance Δ through free space from the exit plane $z = z_0$ to the detector plane $z = z_0 + \Delta$. This could take the form of equations 25 (exact solution), 27 (Fresnel), or 32 (Fraunhofer), depending on various approximations discussed previously. The intensity is then detected as the absolute square of the wave-field at the detector plane, integrated over the acquisition time. Note that while this analysis was performed with respect to an incoming monochromatic wave, the results can easily be extended to a polychromatic wave-field by modeling the frequency-dependent detector response and integrating over all polychromatic components.

I will now begin work to set up a computational framework to generate realistic digital phantoms and apply these various approximate propagators. This will allow me to explore how sensitive the different models are to the object composition and imaging geometry. I have also begun an additional set of notes documenting methods in the literature for linearizing these models for detected intensity with respect to the absorption and accumulated phase imparted to the wave-field by the object (including Paganin, chapter 4). Once I have a good grasp of what sort of approximations are made in the literature, I will perform additional computational studies to evaluate their suitability to our problem.

A Refractive index

We commonly express the refractive index for x-rays as

$$n_\omega = 1 - \delta_\omega + i\beta_\omega, \tag{34}$$

where δ_ω and β_ω are both $\ll 1$ in magnitude. Evaluating $1 - n_\omega^2(x, y, z)$ and keeping only terms to first order in δ_ω and β_ω, we have

$$1 - n_\omega^2(x, y, z) \approx 2\left[\delta_\omega(x, y, z) - i\beta_\omega(x, y, z)\right]. \tag{35}$$

To evaluate this approximation, we can express the complex index of refraction in terms of physical parameters for

some material i:

$$n_\omega^{(i)} \approx 1 - \frac{n_a^{(i)} r_e \lambda_\omega^2}{2\pi} \left(f_{1,\omega}^{(i)} - i f_{2,\omega}^{(i)} \right). \tag{36}$$

where n_a is the atomic number density of the material, r_e is the classical electron radius, λ is the x-ray wavelength, and f_1 and f_2 are the atomic form factors tabulated by NIST.[3]

We thus have

$$\delta_\omega^{(i)} = \frac{n_a^{(i)} r_e \lambda_\omega^2}{2\pi} f_{1,\omega}^{(i)} \qquad \beta_\omega^{(i)} = \frac{n_a^{(i)} r_e \lambda_\omega^2}{2\pi} f_{2,\omega}^{(i)}. \tag{37}$$

Note that we can calculate the atomic number density from the physical density ρ and molar mass M_a:

$$n_a^{(i)} = \frac{\rho^{(i)} N_a}{M_a^{(i)}}, \tag{38}$$

where N_a is Avogadro's number. Using nominal values for all physical parameters, the real and complex components of the index of refraction are shown in Figure 3 for osmium and uranium. We see that both metals have both components $< 10^{-3}$ for relevant energy ranges, so the approximation in equation 35 is valid.

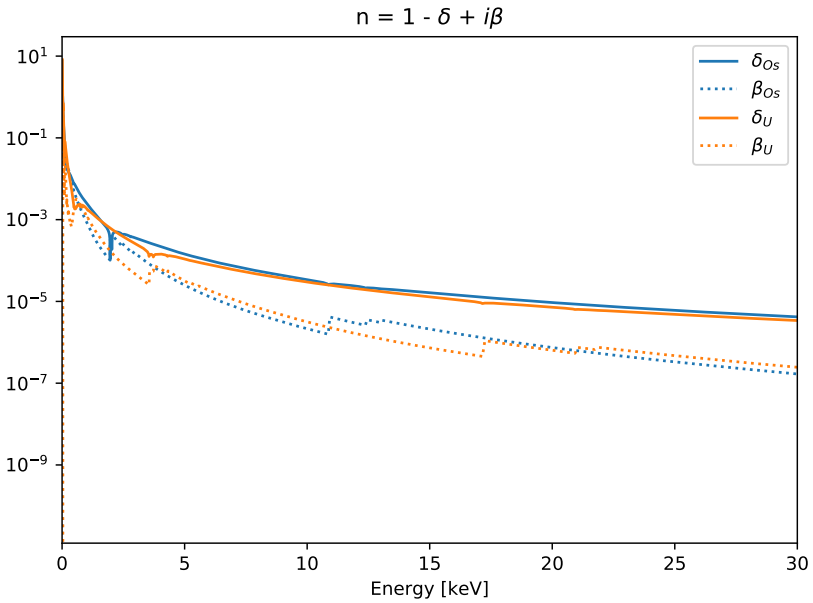

Figure 3: Real (solid) and imaginary (dashed) components of the complex index of refraction for osmium and uranium.

This formulation allows us to redefine our object as the real distribution of physical or atomic densities, after decomposing the object into a set of known materials (osmium and uranium, for instance).

[3] Most derivations I have seen for the tabulated form factors assume a soft x-ray regime, but I believe it also remains valid for small-angle scattering in the hard x-ray regime (see [2]). We are already making the paraxial approximation, so this might be ok, but I want to look a bit deeper into where this expression comes from to be sure. NIST also has extensive documentation on the limitations and uncertainties in different energy regimes, which I will review.

As an example, consider the projection approximation in equation 7. This can be written as:

$$\begin{aligned}\tilde{\psi}_\omega(x,y,z_0) &\approx \exp\left\{-ik\int_0^{z_0}\left[\delta_\omega(x,y,z)-i\beta_\omega(x,y,z)\right]\mathrm{d}z\right\}\tilde{\psi}_\omega(x,y,0)\\ &\approx \exp\left\{-ik\left(\frac{r_e\lambda_\omega^2}{2\pi}\right)\int_0^{z_0}\sum_i^N\left[\left(f_{1,\omega}^{(i)}-if_{2,\omega}^{(i)}\right)n_a^{(i)}(x,y,z)\right]\mathrm{d}z\right\}\tilde{\psi}_\omega(x,y,0)\\ &\approx \exp\left\{-ir_e\lambda_\omega\int_0^{z_0}\sum_i^N\left[\left(f_{1,\omega}^{(i)}-if_{2,\omega}^{(i)}\right)n_a^{(i)}(x,y,z)\right]\mathrm{d}z\right\}\tilde{\psi}_\omega(x,y,0).\end{aligned} \tag{39}$$

B Fourier Transform

Note that in these notes I am using the same convention as Paganin for the 2D Fourier transform:

$$F(k_x,k_y)=\mathcal{F}f(x,y)=\frac{1}{2\pi}\iint_{-\infty}^{\infty}f(x,y)\exp\left[-i(k_xx+k_yy)\right]\mathrm{d}x\mathrm{d}y \tag{40}$$

$$f(x,y)=\mathcal{F}^{-1}F(k_x,k_y)=\frac{1}{2\pi}\iint_{-\infty}^{\infty}F(k_x,k_y)\exp\left[i(k_xx+k_yy)\right]\mathrm{d}k_x\mathrm{d}k_y \tag{41}$$

References

[1] D. M. Paganin, *Coherent X-Ray Optics*. Oxford Science Publications, 2006.

[2] J. Kirz, C. Jacobsen, and M. Howells, "Soft X-ray microscopes and their biological applications," *Quarterly Reviews of Biophysics*, vol. 28, p. 33, feb 1995.